

## Methods

The calculations were performed with JAGUAR 4.1,<sup>[20a]</sup> following previously established procedures.<sup>[11, 12, 14]</sup> The calculations utilized the hybrid B3LYP density functional and the double zeta basis set, LACVP(Fe)/6-31G(C,H,N,O). Geometries were optimized and characterized by frequency calculations. To consider the pure environmental effect, the calculations (with hydrogen bonding and with  $\epsilon = 5.7$ ) did not involve geometry re-optimization. The ZPEs (calculated with the more accurate Gaussian98 routine<sup>[20b]</sup>) of the bare systems were added to the total energies for the different conditions in Figure 2.

Received: March 20, 2002 [Z18940]

- [1] *Cytochrome P450: Structure, Mechanisms and Biochemistry*, 2nd ed. (Ed.: P. R. Ortiz de Montellano), Plenum, New York, **1995**.
- [2] J. T. Groves, Y.-Z. Hang in *Cytochrome P450: Structure, Mechanisms and Biochemistry*, 2nd ed. (Ed.: P. R. Ortiz de Montellano), Plenum, New York, **1995**, chap. 1, p. 3.
- [3] W.-D. Woggon, *Top. Curr. Chem.* **1996**, *184*, 39–95.
- [4] M. Sono, M. P. Roach, E. D. Coulter, J. H. Dawson, *Chem. Rev.* **1996**, *96*, 2841–2887.
- [5] B. Meunier, J. Bernadou, *Struct. Bonding* **2000**, *97*, 3–35.
- [6] S. Yoshioka, S. Takahashi, K. Ishimori, I. Morishima, *J. Inorg. Biochem.* **2000**, *81*, 141–151.
- [7] T. L. Poulos, J. C. Vickery, H. Li in *Cytochrome P450: Structure, Mechanisms and Biochemistry*, 2nd ed. (Ed.: P. R. Ortiz de Montellano), Plenum, New York, **1995**, chap. 4, p. 125.
- [8] a) R. E. White, J. T. Groves, G. A. McClusky, *Acta Biol. Med. Ger.* **1975**, *38*, 475–482; b) R. T. Ruettinger, A. J. Fulco, *J. Biol. Chem.* **1981**, *256*, 5728–5734.
- [9] E. J. Mueller, P. J. Lioda, S. G. Sligar in *Cytochrome P450: Structure, Mechanisms and Biochemistry*, 2nd ed. (Ed.: P. R. Ortiz de Montellano), Plenum, New York, **1995**, chap. 3, p. 83.
- [10] J. J. Devos, O. Sibbeseb, Z. Zhang, P. R. Ortiz de Montellano, *J. Am. Chem. Soc.* **1997**, *119*, 5489–5498.
- [11] F. Ogliaro, N. Harris, S. Cohen, M. Filatov, S. P. de Visser, S. Shaik, *J. Am. Chem. Soc.* **2000**, *122*, 8977.
- [12] S. P. de Visser, F. Ogliaro, N. Harris, S. Shaik, *J. Am. Chem. Soc.* **2001**, *123*, 3037.
- [13] S. Shaik, M. Filatov, D. Schröder, H. Schwarz, *Chem. Eur. J.* **1998**, *4*, 193–198.
- [14] F. Ogliaro, S. Cohen, S. P. de Visser, S. Shaik, *J. Am. Chem. Soc.* **2000**, *122*, 12892.
- [15] T. Ohno, N. Suzuki, T. Dokoh, Y. Urano, K. Kikuchi, M. Hirobe, T. Higuchi, T. Nagano, *J. Inorg. Biochem.* **2000**, *82*, 123–125.
- [16] A. D. N. Vaz, D. F. McGinnity, M. J. Coon, *Proc. Natl. Acad. Sci. USA* **1998**, *95*, 3555–3560.
- [17] A pioneering study of the effect of the protein electric field on the resting state of P450 is given in: D. Harris, G. Loew, *J. Am. Chem. Soc.* **1993**, *115*, 8775–8779.
- [18] D. L. Harris, *Curr. Opin. Chem. Biol.* **2001**, *5*, 724–735.
- [19] R. Weiss, D. Mandon, T. Wolter, A. X. Trautwein, M. Muther, B. Eckhard, A. Gold, K. Jayaray, J. Turner, *J. Biol. Inorg. Chem.* **1996**, *1*, 377.
- [20] a) Jaguar 4.1. Portland OR, **1998**; b) Gaussian98 (Revision A.7), M. J. Frisch, G. W. Trucks, H. B. Schlegel, G. E. Scuseria, M. A. Robb, J. R. Cheeseman, V. G. Zakrzewski, J. A. Montgomery, R. E. Stratmann, J. C. Burant, S. Dapprich, J. M. Millam, A. D. Daniels, K. N. Kudin, M. C. Strain, O. Farkas, J. Tomasi, V. Barone, M. Cossi, R. Cammi, B. Mennucci, C. Pomelli, C. Adamo, S. Clifford, J. Ochterski, G. A. Petersson, P. Y. Ayala, Q. Cui, K. Morokuma, D. K. Malick, A. D. Rabuck, K. Raghavachari, J. B. Foresman, J. Cioslowski, J. V. Ortiz, B. B. Stefanov, G. Liu, A. Liashenko, P. Piskorz, I. Komaromi, R. Gomperts, R. L. Martin, D. J. Fox, T. Keith, M. A. Al-Laham, C. Y. Peng, A. Nanayakkara, C. Gonzalez, M. Challacombe, P. M. W. Gill, B. G. Johnson, W. Chen, M. W. Wong, J. L. Andres, M. Head-Gordon, E. S. Replogle, J. A. Pople, Gaussian, Inc., Pittsburgh, PA, **1998**.

## A Dynamic Rearrangement of a Metal Cluster in a Process that Closely Resembles the Hopping Mechanism of Adatom Diffusion on Metal Surfaces\*\*



Richard D. Adams,\* Burjor Captain, Wei Fu, Perry J. Pellechia, and Mark D. Smith

It has been over 20 years since Muetterties proposed the widely discussed cluster–surface analogy as a model for understanding surface phenomena on an atomic level.<sup>[1–5]</sup> Over the years, however, there have been surprisingly few well-characterized experimental confirmations of this concept.<sup>[6–8]</sup> One important surface process that has been well studied over the years is that known as adatom diffusion.<sup>[9–12]</sup> Adatom diffusion is important to understanding crystal and thin-film growth, phase transitions, segregation, cluster nucleation, and other surface phenomena. The two most important mechanisms are atom hopping and atom exchange.<sup>[9–11]</sup>

In the atom hopping mechanism, an adatom moves from one hollow site to another by moving over a pair of atoms via an “edge bridge” twofold transition state, see the fourfold, twofold, fourfold example in Figure 1.

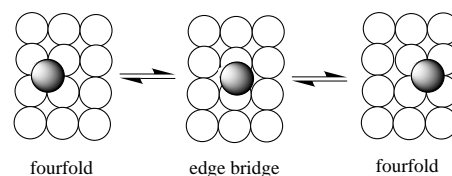


Figure 1. The shaded surface adatom moves from one fourfold site to another via an edge-bridging transition state.

Here we report the synthesis and molecular structures of the compound  $[\text{PtRu}_5(\text{CO})_{15}(\text{PtBu}_3)(\text{C})]$  (**1**) and a study of its unusual molecular dynamics in solution by variable temperature NMR spectroscopy.<sup>[13]</sup> Compound **1** was obtained in 52 % yield from the reaction of  $[\text{Ru}_5(\text{CO})_{15}(\text{C})]$ <sup>[14]</sup> with  $[\text{Pt}(\text{PtBu}_3)_2]$ <sup>[15]</sup> at 25 °C.<sup>[16]</sup> The compound crystallizes in three different crystal modifications depending on the solvent that is used. Mixtures of a triclinic form and a monoclinic form **A** were observed to form by crystallization from solutions in benzene/octane solvent mixtures.<sup>[17, 18]</sup> The molecular structure of the compound is similar in both of these crystal forms and the structure consists of a square-pyramidal cluster of five ruthenium atoms with one platinum atom spanning the square base with significant bonding to the four proximate ruthenium atoms (Figure 2). The four Pt–Ru distances range from

[\*] Dr. R. D. Adams, B. Captain, W. Fu, Dr. P. J. Pellechia, Dr. M. D. Smith  
Department of Chemistry and Biochemistry and USC Nanocenter  
University of South Carolina  
Columbia, SC 29208 (USA)  
Fax: (+1) 803-777-6781  
E-mail: Adams@mail.chem.sc.edu

[\*\*] This work was supported by the Office of Basic Energy Sciences, US Department of Energy.

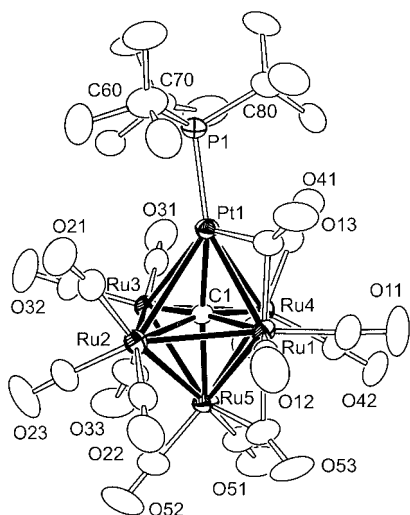


Figure 2. The molecular structure of **1** as found in the triclinic crystal form. Selected bond lengths [Å]: Pt1–Ru1 2.7966(5), Pt1–Ru3 3.1413(5), Pt1–Ru4 3.1463(5), Pt1–Ru2 3.1483(6), Ru1–Ru2 2.9280(7), Ru1–Ru4 2.9297(7), Ru2–Ru3 2.8585(7), Ru3–Ru4 2.8576(7).

2.7966(5)–3.1483(6) Å. A carbido ligand lies inside the cluster of six metal atoms. The single tri-*tert*-butylphosphane ligand coordinates to the platinum atom.

A second monoclinic form **B** was obtained from crystallization by using diethyl ether as the solvent.<sup>[18, 19]</sup> In this crystalline form there are two independent complete molecules. Both are structurally similar, and a diagram of the molecular structure of one of these molecules is shown in Figure 3. In this crystalline state the compound has assumed

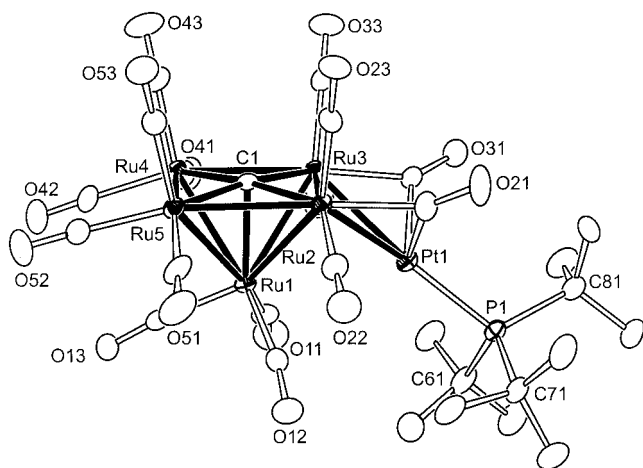


Figure 3. The molecular structure of **1** as found in the monoclinic crystal form **B**. There are two independent molecules in the crystal. Selected interatomic distances [Å] for molecule 1: Pt1–Ru3 2.7894(5), Pt1–Ru2 2.8018(5), Pt1...Ru1 3.3076(5); for molecule 2 (not shown): Pt11–Ru12 2.8213(5), Pt11–Ru13 2.8282(5), Pt11...Ru11 3.1603(5), Ru2–Ru3 2.8928(6), Ru2–Ru5 2.8355(6), Ru3–Ru4 2.8407(7), Ru4–Ru5 2.8726(6).

an isomeric structure in which the platinum atom has moved off the square base to an edge of the cluster of ruthenium atoms (that is, the platinum atom is bonded primarily to only two ruthenium atoms, for molecule 1: Ru3 and Ru2; for molecule 2: Ru12 and Ru13). As indicated by the interatomic

distances Pt1–Ru1 = 3.3076(5) Å and Pt11–Ru11 = 3.1603(5) Å, there may also be some weak bonding between the platinum atom and the ruthenium atom at the apex of the Ru<sub>5</sub> square pyramid.

Interestingly, the <sup>31</sup>P NMR spectrum of **1** in [D<sub>8</sub>]toluene solution at –40 °C shows two phosphorus resonance signals,  $\delta$  = 118.2 and 92.7 ppm, both of which exhibit large coupling to platinum (<sup>195</sup>Pt, 33 % natural abundance), which indicates that both isomers exist in equilibrium in solution and that the phosphorus atom is bonded directly to a platinum atom in each case. The equilibrium is temperature dependent and favors the isomer with the resonance at  $\delta$  = 118.2 ppm as the temperature is lowered below –40 °C. For this equilibrium  $\Delta H^\circ$  = –1.4(1) kcal mol<sup>–1</sup>;  $\Delta S^\circ$  = –6.1(3) cal mol<sup>–1</sup> K<sup>–1</sup>. Most interestingly, as the temperature is raised above –40 °C, the resonances broaden, coalesce, and average into a single resonance,  $\delta$  = 103.9 ppm, with appropriate coupling to platinum at 40 °C. This line broadening indicates that the isomers are interconverting rapidly on the NMR timescale. From computer line-shape simulations it was possible to determine the rates of interconversion at the various temperatures, and in turn, determine the thermodynamic activation parameters:  $\Delta H^\ddagger$  = 8.8(5) kcal mol<sup>–1</sup>;  $\Delta S^\ddagger$  = –8.4 cal mol<sup>–1</sup> K<sup>–1</sup>, (Figure 4).<sup>[20]</sup> The mechanism of interconversion involves a

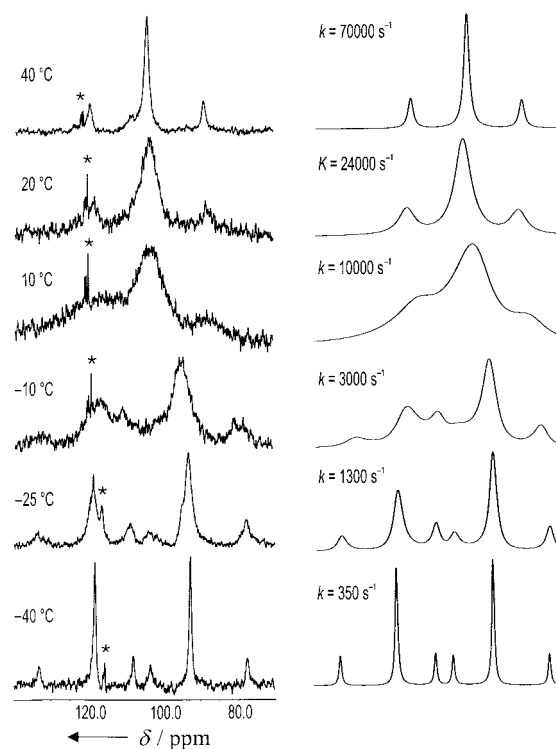


Figure 4. Left: <sup>31</sup>P NMR spectra of compound **1** at various temperatures in [D<sub>8</sub>]toluene solvent. Signals labeled \* are unidentified impurities. Right: computer-simulated spectra at various exchange rates, *k*.

reversible breaking and making of two Pt–Ru bonds with a shift of the platinum–phosphane grouping back and forth between the fourfold Ru<sub>4</sub> site and the twofold edge-bridging Ru<sub>2</sub> site, and it occurs at a rate of 24000 sec<sup>–1</sup> at 20 °C (Figure 5).

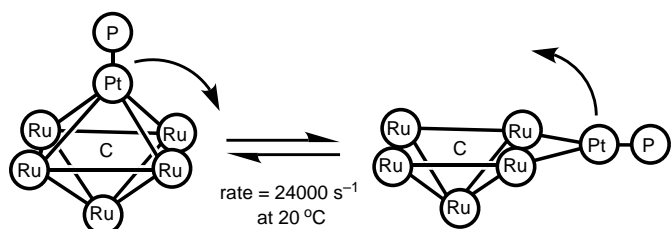


Figure 5. Interconversion of the Pt center between a fourfold and a twofold site.

The great facility of the transformation can be explained by the participation of the CO ligands that help to stabilize the open cluster through their bridging coordination to the platinum atom. Our studies of this molecular cluster model system provide an interesting and unusual new perspective of rearrangements involving the making and breaking of metal–metal bonds in polynuclear metal complexes and by analogy also of the corresponding types of transformations that occur on metal surfaces.

Received: March 11, 2002 [Z18863]

- [1] E. L. Muetterties, *Chem. Rev.* **1979**, 79, 93.
- [2] E. L. Muetterties, *Chem. Soc. Rev.* **1982**, 11, 283.
- [3] E. L. Muetterties, *Surv. Prog. Chem.* **1983**, 10, 61.
- [4] M. R. Albert, J. T. Yates, Jr., *The Surface Scientist's Guide to Organometallic Chemistry*, American Chemical Society, Washington, DC, **1987**.
- [5] X. Xu, N. Wang, Q. Zhang, *Bull. Chem. Soc. Jpn.* **1996**, 69, 529.
- [6] C. M. Friend, *Chem. Rev.* **1992**, 92, 491.
- [7] S. Brait, S. Deabate, S. A. R. Knox, E. Sappa, *J. Cluster Sci.* **2001**, 12, 139.
- [8] D. B. Brown, B. F. G. Johnson, C. M. Martin, A. E. H. Wheatley, *J. Chem. Soc. Dalton Trans.* **2000**, 2055.
- [9] T. T. Tsong, *Prog. Surf. Sci.* **2001**, 67, 235.
- [10] G. L. Kellogg, *Surf. Sci. Rep.* **1994**, 21, 1.
- [11] C. M. Chang, C. M. Wei, J. Hafner, *J. Phys. Condens. Matter* **2001**, 13, L321.
- [12] A. Zangwill, *Physics at Surfaces*, Cambridge University Press, Cambridge, **1988**.
- [13] *Dynamic Nuclear Magnetic Resonance Spectroscopy*, (Eds.: L. M. Jackman, F. A. Cotton), Academic Press, New York, **1975**.
- [14] P. J. Dyson, *Adv. Organomet. Chem.* **1999**, 43, 43.
- [15] S. Otsuka, T. Yoshida, M. Matsumoto, K. Nakatsu, *J. Am. Chem. Soc.* **1976**, 98, 5850.
- [16]  $[\text{Ru}_5(\text{CO})_{15}(\mu_6\text{-C})]$  (18.0 mg) was allowed to react with  $[\text{Pt}(\text{PrBu}_3)_2]$  (10.5 mg) in  $\text{CH}_2\text{Cl}_2$  (15 mL) under a nitrogen atmosphere at room temperature for 30 min. The product was isolated by TLC to yield 13.2 mg (52 %) of red crystals of  $[\text{Ru}_5\text{Pt}(\text{CO})_{15}(\text{PrBu}_3)(\mu_6\text{-C})]$  (**1**). Spectral data for **1**: IR  $\nu_{\text{CO}}$  (in  $\text{CH}_2\text{Cl}_2$ ):  $\tilde{\nu} = 2087$  (m), 2055 (s), 2033 (s), 2028 (s), 1991 (sh),  $1822\text{ cm}^{-1}$  (w, br);  $^{31}\text{P}\{^1\text{H}\}$  NMR ( $-40^\circ\text{C}$ ,  $[\text{D}_8]\text{toluene}$ , 202.5 MHz):  $\delta = 118.2$  ( $^1J_{\text{Pt-P}} = 5983$  Hz),  $\delta = 92.7$  ppm ( $^1J_{\text{Pt-P}} = 6164$  Hz); elemental analysis (%) calcd: C 25.19, H 2.02; found: C 25.28, H 1.92.
- [17] Crystal data for **1** in triclinic form:  $\text{PtRu}_5\text{PO}_{15}\text{C}_{28}\text{H}_{27}$ ,  $M_r = 1334.91$ , space group  $P\bar{1}$ ,  $a = 9.9510(5)$ ,  $b = 12.1523(6)$ ,  $c = 16.8957(8)$  Å,  $\alpha = 79.797(1)^\circ$ ,  $\beta = 87.338(1)^\circ$ ,  $\gamma = 72.9380(10)^\circ$ ,  $V = 6769.1(9)$  Å<sup>3</sup>,  $Z = 2$ ,  $T = 293$  K,  $\text{MoK}\alpha$  radiation,  $\lambda = 0.71073$  Å. The final  $R$  factor  $R_1(F)$  was 0.0384 for 7697 reflections with  $I > 2\sigma(I)$ . Crystal data for **1** in the monoclinic form **A**: space group  $P2_1/n$ ,  $a = 12.4684(10)$ ,  $b = 17.9669(15)$ ,  $c = 17.3482(14)$  Å,  $\beta = 107.613(2)^\circ$ ,  $V = 3704.1(5)$  Å<sup>3</sup>,  $Z = 4$ ,  $T = 190$  K,  $\text{MoK}\alpha$  radiation,  $\lambda = 0.71073$  Å. The final  $R$  factor  $R_1(F)$  was 0.0463 for 5594 reflections with  $I > 2\sigma(I)$ .

- [18] CCDC-181108–181110 contains the supplementary crystallographic data for this paper. These data can be obtained free of charge via [www.ccdc.cam.ac.uk/conts/retrieving.html](http://www.ccdc.cam.ac.uk/conts/retrieving.html) (or from the Cambridge Crystallographic Data Centre, 12, Union Road, Cambridge CB21EZ, UK; fax: (+44) 1223-336-033; or [deposit@ccdc.cam.ac.uk](mailto:deposit@ccdc.cam.ac.uk)).
- [19] Crystal data for **1** in the monoclinic form **B**: space group  $P2_1/c$ ,  $a = 14.1957(12)$ ,  $b = 18.0213(15)$ ,  $c = 29.027(2)$  Å,  $\beta = 92.113(2)^\circ$ ,  $V = 3704.1(5)$  Å<sup>3</sup>,  $Z = 4$ ,  $T = 190$  K,  $\text{MoK}\alpha$  radiation,  $\lambda = 0.71073$  Å. The final  $R$  factor  $R_1(F)$  was 0.0379 for 14877 reflections with  $I > 2\sigma(I)$ .
- [20] Line-shape simulations of the NMR spectra in the exchange-broadened region were performed by using the program EXCHANGE written by R. E. D. McClung, Department of Chemistry, University of Alberta, Edmonton, Alberta, Canada.

## Electronic Structure and Bonding in Hexacoordinate Silyl–Palladium Complexes\*\*

Edward C. Sherer, Christopher R. Kinsinger, Bethany L. Kormos, Jason D. Thompson, and Christopher J. Cramer\*

Trimerization of  $[\text{Pd}^{\text{II}}(\text{R}_2\text{PCH}_2\text{CH}_2\text{PR}_2)\{1,2\text{-C}_6\text{H}_4(\text{SiH}_2)_2\}]$  (**1**; where  $\text{R} = \text{Me}$  or  $\text{Et}$ ) has been demonstrated to produce a trinuclear complex **2** where two of the Pd atoms can be readily characterized as  $\text{Pd}^{\text{II}}$  centers but the nature of the third, central Pd atom is less clear (Scheme 1, by-products not shown).<sup>[1]</sup> While this Pd atom (Pd1) is drawn in Scheme 1 as bonding directly to two Si atoms and further interacting with two Si–Si bonds, the interatomic distances from the X-ray crystal-structure data could also be interpreted to be consistent with an absence of Si–Si bonds and instead six Pd–Si bonds,<sup>[1]</sup> that is, the central metal would formally be  $\text{Pd}^{\text{VI}}$ . Both structures are without precedent in palladium coordination chemistry,<sup>[2, 3]</sup> although compounds of  $\text{Pd}^{[4-7]}$  and  $\text{Pt}^{[8, 9]}$  have been reported for inorganic compounds of the form  $[\text{MF}_n]$  ( $\text{M} = \text{Pd}, \text{Pt}$ ;  $n = 2, 4, 6$ ), where the extreme electronegativity of fluorine is exploited for the generation of higher oxidation states.<sup>[10]</sup>

To better understand the nature of the bonding in **2**, we have carried out DFT calculations on **2** and relevant model compounds. With the exception of single-point calculations using the X-ray geometries of **2a** and **2b**, all the structures were fully optimized and verified as minima by analytic frequency calculations. The functional employed was of the hybrid variety<sup>[11]</sup> and combined exact Hartree–Fock exchange with the gradient-corrected exchange and correlation functionals of Becke<sup>[12]</sup> and Lee, Yang, and Parr,<sup>[13]</sup> respec-

[\*] Prof. Dr. C. J. Cramer, E. C. Sherer, C. R. Kinsinger, B. L. Kormos, J. D. Thompson  
Department of Chemistry and Supercomputing Institute  
University of Minnesota  
207 Pleasant Street SE, Minneapolis, MN 55455-0431 (USA)  
Fax: (+1) 612-626-2006  
E-mail: [cramer@chem.umn.edu](mailto:cramer@chem.umn.edu)

[\*\*] Support from the National Science Foundation (CHE-9876792) is gratefully acknowledged.